TTK-15-32

Prospects of constraining the Higgs CP nature in the tau decay channel at the LHC

Stefan Berge[1], **Werner Bernreuther**[2] **and Sebastian Kirchner**[3]

Institut für Theoretische Teilchenphysik und Kosmologie,
RWTH Aachen University, 52056 Aachen, Germany

arXiv:1510.03850v1 [hep-ph] 13 Oct 2015

Abstract

We investigate how precisely the CP nature of the 125 GeV Higgs boson h, parametrized by a scalar-pseudoscalar Higgs mixing angle ϕ_τ, can be determined in $h \to \tau^-\tau^+$ decay with subsequent τ-lepton decays to charged prongs at the Large Hadron Collider (LHC). We combine two methods in order to define an observable φ^*_{CP} which is sensitive to ϕ_τ: We use the ρ-decay plane method for $\tau^\mp \to \rho^\mp$ and the impact parameter method for all other major τ decays. For estimating the precision with which ϕ_τ can be measured at the LHC (13 TeV) we take into account the $\tau^-\tau^+$ background from Drell-Yan production and perform a Monte Carlo simulation of measurement uncertainties on the φ^*_{CP} signal and background distributions. We obtain that the mixing angle ϕ_τ can be determined with an uncertainty of $\Delta\phi_\tau \simeq 15^\circ$ (9°) at the LHC with an integrated luminosity of $150\,\text{fb}^{-1}$ ($500\,\text{fb}^{-1}$), and with $\Delta\phi_\tau \approx 4^\circ$ with $3\,\text{ab}^{-1}$. Future measurements of ϕ_τ yield direct information on whether or not there is an extended Higgs-boson sector with Higgs-sector CP violation. We analyze this in the context of a number of two-Higgs-doublet extensions of the Standard Model, namely the so-called aligned model and conventional two-Higgs-doublet extensions with tree-level neutral flavor conservation.

PACS numbers: 11.30.Er, 12.60.Fr, 14.80.Bn

Keywords: Higgs boson, Higgs sector extensions, CP violation, tau leptons, spin correlations

[1] berge@physik.rwth-aachen.de

[2] breuther@physik.rwth-aachen.de

[3] kirchner@physik.rwth-aachen.de

I. INTRODUCTION

The investigations of the production and decay modes of the $h(125\text{GeV})$ spin-zero resonance, which was discovered at the Large Hadron Collider (LHC) in 2012 [1, 2], show that the properties of this particle are compatible [3, 4] with those of the Standard Model (SM) Higgs boson. In particular, the analysis of angular correlations in $h \to ZZ, W^+W^-$ excluded that h is a pseudoscalar state ($J^P = 0^-$) [5, 6]. However, the results of [5, 6] do not imply that h is purely CP-even ($J^P = 0^+$), because a pseudoscalar component of h is most likely not detectable in its decays to weak gauge bosons.

The exploration whether or not $h(125\text{GeV})$ is a pure CP-even state is of prime interest. If a CP-odd component of h would be detected, that is, if h would turn out to be a CP mixture, it would be evidence of new physics, i.e., of non-standard CP violation. One way to probe the CP nature of h is to measure $\tau\tau$ spin correlations in $h \to \tau^+\tau^-$. Respective phenomenological investigations for h production and decay to τ leptons at the LHC include [7–14]. Because the $\tau^+\tau^-$ zero-momentum frame (ZMF) and the $\tau^\pm$ rest frames cannot be experimentally reconstructed at the LHC, the central aspect of these analyses is to define an alternative inertial frame and to construct an observable in this frame which allows to discriminate with high sensitivity between a CP-even, CP-odd, and a CP-mixed Higgs boson h. The method proposed and applied in [8, 9, 13, 15] is applicable to all subsequent $\tau^\pm$ decays into 1 or 3 charged prongs. It requires the measurement of the energy and 3-momentum of the charged prong (which in our case is either a charged lepton or a charged pion) and its impact parameter in the laboratory frame. We will call this approach the impact parameter method in the following. Another method, which we will call the ρ-decay plane method, was first proposed and applied in [16–20] for Higgs-boson production and decay to $\tau^+\tau^-$ in e^+e^- collisions. The method works only for subsequent τ decays to charged ρ mesons and requires the measurement of the 4-momenta of the charged and neutral pion from $\rho^\pm$ decay. This method was analyzed in [10, 11, 14] for Higgs-boson production at the LHC and shows a better sensitivity to scalar-pseudoscalar Higgs mixing than the impact parameter method applied to $\tau \to \rho$ decays.

The aim of this paper is to combine both methods. We apply a slight variant of the ρ-decay plane method to $\tau^\pm \to \rho^\pm$ and the impact parameter method of [8, 9, 13, 15] to the other major 1- and 3-prong τ decays and define a discriminating variable for probing the CP nature of h. We analyze in this way all major τ decays into one and three charged prongs. We estimate the statistical uncertainty with which the scalar-pseudoscalar Higgs mixing angle ϕ_τ defined below can eventually be measured at the LHC (13 TeV) with this approach. Assuming that this precision on ϕ_τ can be reached, we investigate its impact on the parameters of a number of Standard Model extensions with non-standard CP violation, in particular Higgs-sector

CP violation, namely the so-called aligned two-Higgs-doublet model [21] and conventional two-Higgs-doublet models with neutral flavor conservation but Higgs-sector CP violation at tree-level.

In this paper we consider the production of the Higgs boson $h(125\text{GeV})$ at the LHC with 13 TeV center-of-mass energy and its subsequent decay into a pair of τ leptons:

$$pp \to h + X \to \tau^- \tau^+ + X. \tag{1}$$

The analysis of this paper can be applied to any h production mode. For definiteness we shall consider below Higgs production by gluon gluon fusion. The general model-independent effective Yukawa interactions of h with τ leptons can be parametrized as follows:

$$\mathscr{L}_Y = -\frac{m_\tau}{\mathrm{v}}\, \kappa_\tau \left(\cos\phi_\tau \bar{\tau}\tau + \sin\phi_\tau \bar{\tau} i\gamma_5 \tau\right) h\,, \tag{2}$$

where $\mathrm{v} = 246$ GeV, $\kappa_\tau > 0$ denotes the reduced Yukawa coupling strength, and the angle ϕ_τ parametrizes the amount of CP violation in the $h\tau\tau$ interaction. Henceforth, we will call ϕ_τ the scalar-pseudoscalar Higgs mixing angle. At this point we recall the following terminology. We call a neutral Higgs boson to be a CP-even or scalar state (CP-odd or pseudoscalar state) if it couples – also beyond the tree level – only to scalar (pseudoscalar) fermion currents. If the Higgs boson couples to both currents we call it a CP mixture.

As already mentioned above, we analyze all major 1- and 3-prong tau decay modes:

$$\tau \to l + \nu_l + \nu_\tau\,, \tag{3}$$

$$\tau \to a_1 + \nu_\tau \to \pi + 2\pi^0 + \nu_\tau\,, \tag{4}$$

$$\tau \to a_1^{L,T} + \nu_\tau \to 2\pi^\pm + \pi^\mp + \nu_\tau\,, \tag{5}$$

$$\tau \to \rho + \nu_\tau \to \pi + \pi^0 + \nu_\tau\,, \tag{6}$$

$$\tau \to \pi + \nu_\tau\,. \tag{7}$$

We call the decay mode $\tau \to a_1^{L,T} + \nu_\tau$ in (5) also '1-prong', because the 4-momentum of $a_1^\pm$ can be obtained from the measured 4-momenta of the 3 charged pions. The longitudinal (L) and transverse (T) helicity states of the a_1 resonance can be separated by using known kinematic distributions [22–25].

In the following we denote the final charged particles by $a^-, a'^+ \in \{e^\pm, \mu^\pm, \pi^\pm, a_1^{L,T,\pm}\}$. The normalized distributions of polarized $\tau^\mp$ decays to $a^\mp$ are, in the $\tau^\mp$ rest frame, of the form:

$$\Gamma_a{}^{-1} \mathrm{d}\Gamma_a \left(\tau^\mp(\hat{\mathbf{s}}^\mp) \to a^\mp(q^\mp) + X\right) = n\left(E_\mp\right)\left[1 \pm b\left(E_\mp\right)\hat{\mathbf{s}}^\mp \cdot \hat{\mathbf{q}}^\mp\right] dE_\mp \frac{d\Omega_\mp}{4\pi}\,. \tag{8}$$

Here, $\hat{\mathbf{s}}^\mp$ are the normalized spin vectors of the $\tau^\mp$ and $E\mp$ and $\hat{\mathbf{q}}^\mp$ are the energies and unit 3-momenta of $a^\mp$ in the respective τ rest frame. The spectral functions n and b are given, for instance, in [9]. The function $b(E_\mp)$ contains the information on the τ-spin analyzing power

of the particle $a^{\mp}$. We recall that the τ-spin analyzing power is maximal for the direct decays to pions, $\tau^{\mp} \to \pi^{\mp}$, and for $\tau^{\mp} \to a_1^{L,T,\mp}$. (The τ-spin analyzing power of a_1^{L-} and a_1^{T-} is $+1$ and -1, respectively.) For the other decays, the τ-spin analyzing power of $l^{\mp}$ and $\pi^{\mp}$ depends on the energy of these particles. It can be enhanced by appropriately chosen energy cuts.

The paper is organized as follows. In Sec. II we first review the impact parameter method of [8, 9, 13, 15]. Then we introduce a slightly modified version of the ρ-decay plane method [16–20] which allows to combine both methods for those $\tau^-\tau^+$ decays where one τ lepton decays to $\rho + \nu_\tau$ and the other one to a charged prong $a \neq \rho$. We define an angle φ^*_{CP} with which one can probe, with this combined method and for all $\tau^-\tau^+$ decay modes listed above, whether or not h has a CP-violating coupling to the τ lepton. Moreover, we define an asymmetry [13, 15] that is useful in estimating the error $\Delta\phi_\tau$ with which the mixing angle ϕ_τ can be measured in each $\tau^-\tau^+$ decay channel. In Sec. III we apply the combined method introduced in the previous section to the $h \to \tau\tau$ decay modes listed above, at the LHC (13 TeV). We take into account the irreducible background from Drell-Yan production, $\gamma^*/Z^* \to \tau^-\tau^+$, apply acceptance cuts and account for measurement uncertainties by Monte Carlo simulation[4] as in [13]. We estimate the precision with which the mixing angle ϕ_τ can eventually be measured at the LHC (13 TeV). In Sec. IV we investigate the impact this precision on ϕ_τ and the expected precision on the reduced Yukawa coupling strength κ_τ would have on the parameters of Standard Model extensions with non-standard CP violation, in particular Higgs-sector CP violation. We confine ourselves to non-supersymmetric two-Higgs-doublet extensions. First we analyze the so-called aligned two-Higgs-doublet model [21] and then discuss conventional two-Higgs-doublet models (2HDM) with tree-level neutral flavor conservation and a CP-violating tree-level Higgs potential, namely the type-I and type-II 2HDM, the flipped, and the lepton specific model. Finally, we add a short remark on the so-called inert model. We conclude in Sec. V.

II. OBSERVABLES

In the decay $h \to \tau\tau$ the information on the scalar-pseudoscalar mixing angle ϕ_τ is encoded in the spin-spin correlation of the $\tau^+\tau^-$ leptons. For $\beta_\tau = \sqrt{1-4m_\tau^2/m_h^2} \approx 1$ the differential decay width is proportional to (cf., for instance [9])

$$\begin{aligned} d\Gamma_{h\to\tau^+\tau^-} \propto\ & 1 - s_z^- s_z^+ + \cos(2\phi_\tau)\left(\mathbf{s}_T^- \cdot \mathbf{s}_T^+\right) \\ & + \sin(2\phi_\tau)\left[\left(\mathbf{s}_T^+ \times \mathbf{s}_T^-\right)\cdot \hat{\mathbf{k}}^-\right], \end{aligned} \tag{9}$$

[4] Our own Monte-Carlo simulation program uses the external software packages [26–30].

where $\hat{\mathbf{k}}^-$ is the normalized τ^- 3-momentum in the Higgs-boson rest frame, $\hat{\mathbf{s}}^\mp$ are the unit spin vectors of the $\tau^\mp$ in their respective τ rest frames[5], and $s_z^\mp$ ($\mathbf{s}_T^\mp$) denotes the longitudinal (transverse) component of $\hat{\mathbf{s}}^\mp$ with respect to $\hat{\mathbf{k}}^-$. Eq. (9) shows that, in the Higgs-boson rest frame, information on ϕ_τ is obtained from the correlation of the transverse components of the τ-spins. This correlation is encoded in the distribution of the angle between the plane defined by $\hat{\mathbf{s}}^-$ and $\hat{\mathbf{k}}^-$ and the plane defined by $\hat{\mathbf{s}}^+$ and $\hat{\mathbf{k}}^-$. The τ leptons self-analyze their spin direction through their parity-violating weak decays into charged prongs (cf. (8)). Nevertheless, the angle between the above-mentioned plane cannot be measured directly because the $\tau^\pm$ rest-frames cannot be reconstructed. Yet, the impact parameter method [8, 9, 13, 15] or the ρ-decay plane method [16–20] allows to determine this angle without reconstruction of the 4-momenta of the $\tau^\mp$.

A. Impact parameter method

The method described in [8, 9, 13, 15] can be used for all $\tau^\mp$ decay modes (3) - (7) if the charged prongs prongs a^-, a'^+ have a non-vanishing impact parameter. This method requires the measurement of the 4-momenta of a^- and a'^+ and their impact parameters vectors $\mathbf{n}_\mp$ in the laboratory frame. The vectors $\mathbf{n}_\mp$ begin at the Higgs-boson production vertex (which should be known with some precision also along the beam direction, which we take to be the z direction) and end perpendicular on the a^- and a'^+ tracks. The corresponding unit vectors are denoted by $\hat{\mathbf{n}}_\mp$. The 4-momenta q_-^μ, q_+^μ of a^-, a'^+ and the impact parameter 4-vectors defined by $n_\mp^\mu = (0, \hat{\mathbf{n}}_\mp)$ are boosted into the $a^- a'^+$ ZMF. The variables in the $a^- a'^+$ ZMF are denoted by an asterisk, for instance, $q_\mp^{*\mu}$, $n_\mp^{*\mu}$. An observable that is sensitive to the *CP* nature of the Higgs boson is obtained as follows: We decompose $\mathbf{n}_\mp^*$ into their normalized components $\hat{\mathbf{n}}_{||}^{*\mp}$ and $\hat{\mathbf{n}}_\perp^{*\mp}$ which are parallel and perpendicular to the respective 3-momentum $\mathbf{q}_-^*$ and $\mathbf{q}_+^*$. An unsigned angle φ^* ($0 \le \varphi^* \le \pi$) and a *CP*-odd and *T*-odd triple correlation $\mathscr{O}_{CP}^*$ ($-1 \le \mathscr{O}_{CP}^* \le 1$) can be defined by

$$\varphi^* = \arccos(\hat{\mathbf{n}}_\perp^{*+} \cdot \hat{\mathbf{n}}_\perp^{*-}), \qquad \mathscr{O}_{CP}^* = \hat{\mathbf{q}}_-^* \cdot (\hat{\mathbf{n}}_\perp^{*+} \times \hat{\mathbf{n}}_\perp^{*-}), \tag{10}$$

where $\hat{\mathbf{q}}_-^*$ is the normalized a^- momentum in the $a^- a'^+$ ZMF. Using these two quantities one can define a signed angle φ_{CP}^* [13] between the $\tau^- \to a^-$ and $\tau \to a'^+$ decay planes by

$$\varphi_{CP}^* = \begin{cases} \varphi^* & \text{if } \mathscr{O}_{CP}^* \ge 0, \\ 2\pi - \varphi^* & \text{if } \mathscr{O}_{CP}^* < 0, \end{cases} \tag{11}$$

[5] These τ rest frames are obtained from the Higgs rest frame by a rotation-free Lorentz boost along the $\tau^\pm$ momenta.

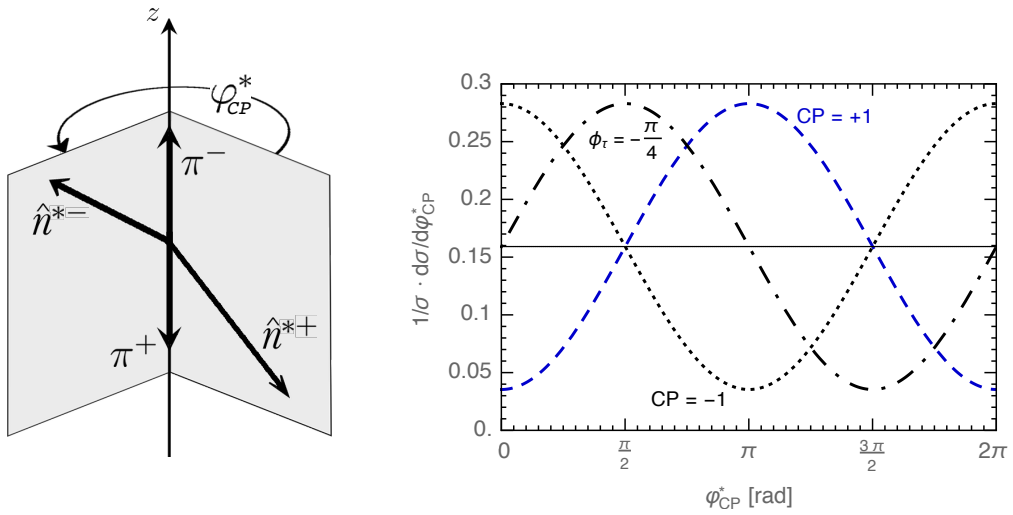

Figure 1. Left: Definition of 3-vectors and the angle φ^*_{CP} in the $a^-a'^+$ ZMF (here $\pi^-\pi^+$ ZMF) for the impact parameter method. Right: Normalized φ^*_{CP} distribution for $pp \to h \to \tau^-\tau^+ \to \pi^-\pi^+ + 2\nu_\tau$ at the LHC (13 TeV) at NLO QCD with $q_T^{\pi\pm} \geq 20$ GeV and $|\eta_{\pi\pm}| < 2.5$, and $m_h = 125$ GeV. The blue dashed, the black dotted and black long-dashed line shows the distribution for a CP-even Higgs boson ($\phi_\tau = 0$), a CP-odd Higgs boson ($\phi_\tau = \pm\pi/2$) and a CP mixture ($\phi_\tau = -\pi/4$), respectively. The solid black flat line is the distribution due to the $Z^*/\gamma^* \to \tau\tau$ background.

and $0 \leq \varphi^*_{CP} \leq 2\pi$. A sketch of the definition of φ^*_{CP} in the $a^-a'^+$ ZMF is given in Fig. 1, left. The distributions of φ^*_{CP} were computed for inclusive Higgs production $ij \to hX$ (where ij denote partons) and subsequent decays $h \to \tau^-\tau^+ \to a^-a'^+$ in [13]. The differential partonic cross section $\hat{\sigma}_{ij}$, integrated over the polar angles of the charged prongs, is proportional to $1 - \pi^2 b(E_-)b(E_+)\cos(\varphi^*_{CP} - 2\phi_\tau)/16$, where the functions $b(E_-)$, $b(E_+)$ defined in (8) contain the information on the τ-spin analyzing power of a^- and a'^+, respectively. From this distribution the Higgs mixing angle ϕ_τ can be extracted.

For the computation of the φ^*_{CP} distributions we use the Monte Carlo program MCFM [31] to generate Higgs-boson production by gluon-gluon fusion at NLO QCD. Using the narrow width approximation we include $h \to \tau^-\tau^+$ with τ spin correlations and the subsequent decays $\tau^-\tau^+ \to a^-a'^+$ with our own Monte Carlo code. As an example, we show in Fig. 1, right, the normalized φ^*_{CP} distribution $pp \to h \to \tau^-\tau^+ \to \pi^-\pi^+ + 2\nu_\tau$ for the LHC for a CP-even and CP-odd Higgs boson and for a CP-mixture.

A possible non-vanishing scalar-pseudoscalar mixing angle ϕ_τ can be extracted from the shift of the measured distribution with respect to the SM prediction (CP-even h, blue dashed line). One can determine ϕ_τ by fitting the function $f = u\cos\left(\varphi^*_{CP} - 2\phi_\tau\right) + \mathrm{w}$ to the measured φ^*_{CP} distributions for the respective final states aa'. The function is constrained by $\int_0^{2\pi} d\varphi^*_{CP} f = 2\pi\mathrm{w} = \sigma_{aa'}$, where $\sigma_{aa'}$ is the h-production cross section including the respective decay

branching fractions. The estimate of the uncertainty of φ^*_{CP} for a given final state depends on the values of the associated parameters u and w. For the comparison of different channels it is convenient to use the following asymmetry [13, 15]:

$$A^{aa'} = \frac{1}{\sigma_{aa'}} \int_0^{2\pi} d\varphi^*_{CP} \left\{ d\sigma_{aa'}(u\cos(\varphi^*_{CP} - 2\phi_\tau) > 0) - d\sigma_{aa'}(u\cos(\varphi^*_{CP} - 2\phi_\tau) < 0) \right\}$$
$$= \frac{-4u}{2\pi \mathrm{w}} . \qquad (12)$$

The values of $A^{aa'}$ are independent of the mixing angle ϕ_τ but do depend on the product of the τ-spin analyzing powers of a and a'. The larger $A^{aa'}$ the smaller the error $\Delta\phi_\tau$ in this decay channel, for a given number of events. The τ-spin analyzing power, and thus $A^{aa'}$, is maximal for the direct decays $\tau^\mp \to \pi^\mp$ and for $\tau^\mp \to a_1^{L,T\mp}$. In case of the decays $\tau^\mp \to l^\mp$, $\tau^\mp \to \rho^\mp \to \pi^\mp$, and $\tau^\mp \to a_1^\mp \to \pi^\mp$ the τ-spin analyzing power of the charged lepton, respectively of the charged pion can be enhanced by applying an appropriate cut on the energy of $l^\mp$ and $\pi^\mp$, respectively.

For the $\tau\tau \to \pi\pi$ decay channel, the asymmetry $A^{\pi\pi} = 39\%$ if no cuts on the pions are applied. While a cut on the rapidities of the charged pions does not change the normalized φ^*_{CP} distribution, rejecting pions with low q_T increases the amplitude u. Applying the cuts $q_T^{\pi\pm} \geq 20$ GeV, and $|\eta_{\pi\pm}| \leq 2.5$ on the final charged pions, as was done in Fig. 1, increases the asymmetry to $A^{\pi\pi} = 50\%$.

The asymmetry $A^{aa'}$ was computed in [13] for all combinations of the τ decay modes (3) - (7) with appropriate cuts. An important feature of the φ^*_{CP} distribution is that the contribution from the irreducible Drell-Yan background $Z^*/\gamma^* \to \tau\tau$ is flat for all charged prongs a, a', as shown in [13]. The Drell-Yan contribution decreases the height of the normalized distribution and thus the magnitude of the asymmetry (12), but is not a major obstacle in extracting the Higgs mixing angle ϕ_τ.

B. Method using the ρ-decay plane

For Higgs-boson production in e^+e^- collisions and the subsequent decay channel $h \to \tau^-\tau^+ \to \rho^-\rho^+ + 2\nu_\tau$, a slightly different method was proposed and analyzed in Refs. [16–20] for determining the scalar-pseudoscalar mixing angle ϕ_τ. This method requires that the tracks of the charged and neutral pion of each ρ decay can be separated. That is, both the charged and the neutral pion momenta must be measured and correctly assigned to $\rho^\mp$. The charged and neutral pion momenta are then boosted into the $\rho^-\rho^+$ ZMF, and the resulting π^-, π^0 and π^+, π^0 3-momenta in this frame define two decay planes. The angle between these planes serves as discriminating variable for determining the CP nature of h. This approach was applied in the recent studies [10, 11, 14] for Higgs-boson production at the LHC.

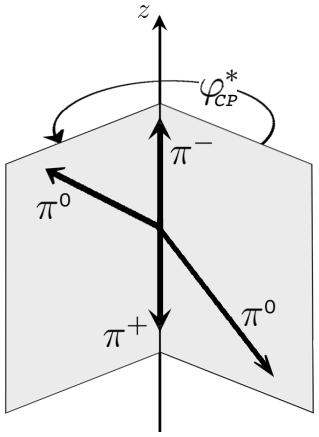

Figure 2. Illustration of φ^*_{CP} in the ρ decay-plane method as defined in (14) for $pp \to h^0 \to \tau^-\tau^+ \to \rho^-\rho^+ + 2\nu$.

Rather than choosing the $\rho^-\rho^+$ ZMF we use in the following, as for the impact parameter method, the $a^-a'^+$ ZMF of the charged pions from $\rho^\mp$ decay. This allows us to standardize the definition of the discriminating variable for both methods. In the remainder of this section we define this variable for the $h \to \tau^-\tau^+ \to \rho^-\rho^+$ decay channel. One boosts the π^-, π^0 and π^+, π^0 4-momenta, measured in the laboratory frame, into the $\pi^-\pi^+$ ZMF. In this frame, we denote the π^-, π^0 (π^+, π^0) 3-momenta by $\mathbf{q}^{*-}, \mathbf{q}^{*0-}$ ($\mathbf{q}^{*+}, \mathbf{q}^{*0+}$). In the $\pi^-\pi^+$ ZMF we compute, for each neutral pion, the normalized vector $\hat{\mathbf{q}}^{*0-}_\perp$ and $\hat{\mathbf{q}}^{*0+}_\perp$ which is transverse to the direction of the associated charged pion. The angle between these two vectors is given by[6]

$$\varphi^* \;=\; \arccos\left(\hat{\mathbf{q}}^{*0+}_\perp \cdot \hat{\mathbf{q}}^{*0-}_\perp\right), \qquad 0 \le \varphi^* \le \pi\,. \tag{13}$$

In order to define a signed angle we use the *CP*-odd triple correlation $\mathscr{O}^*$

$$\mathscr{O}^* \;=\; \hat{\mathbf{q}}^{*-} \cdot \left(\hat{\mathbf{q}}^{*0+}_\perp \times \hat{\mathbf{q}}^{*0-}_\perp\right), \qquad -1 \le \mathscr{O}^* \le +1\,.$$

The discriminating variable that is sensitive to the mixing angle ϕ_τ is defined by

$$\varphi^*_{CP} = \begin{cases} \varphi^* & \text{if } \mathscr{O}^* \ge 0 \\ 2\pi - \varphi^* & \text{if } \mathscr{O}^* < 0 \end{cases}, \qquad \text{with} \quad 0 \le \varphi^*_{CP} \le 2\pi\,. \tag{14}$$

The angle φ^*_{CP} is shown in Fig. 2. In order to obtain a non-trivial φ^*_{CP} distribution, one needs to separate the events into two classes depending on the sign of the $\tau^\mp$ spin-analyzing functions or polarimeter vectors associated with the $\tau^\mp \to \rho^\mp$ decays [16–20]. These polarimeter

[6] In (13) and in (14) we use the same notation as in (10) and (11), respectively, in order not to overload the notation.

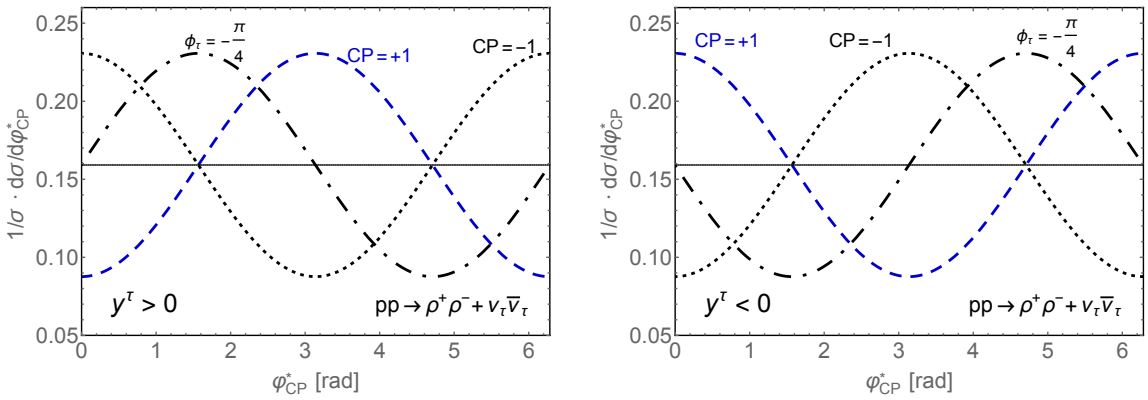

Figure 3. Normalized φ^*_{CP} distribution obtained with the ρ-decay plane method (14) for $pp \to h \to \tau^-\tau^+ \to \rho^-\rho^+ + 2\nu_\tau$ at the LHC (13 TeV). The left and right plots are for events with $y^\tau > 0$ and $y^\tau < 0$, as defined in (15). The cuts $p_T^{\rho\pm} \geq 20$ GeV and $|\eta_{\rho\pm}|, |\eta_{\pi\pm}| \leq 2.5$ were applied. The blue dashed, black dotted, and black long-dashed lines show the distribution for a *CP*-even Higgs boson ($\phi_\tau = 0$), a *CP*-odd Higgs boson ($\phi_\tau = \pm\pi/2$), and a *CP* mixture ($\phi_\tau = -\pi/4$), respectively. The flat lines are the distributions due to Drell-Yan production.

vectors are proportional to $E_{\pi^\pm} - E_{\pi^0}$, where $E_{\pi^\pm}$ and E_{π^0} are the energies of the pions associated with the decays of $\rho^\pm$ in the respective $\tau^\pm$ rest frames. Using the variables

$$y^\tau_- = \frac{(E_{\pi^-} - E_{\pi^0})}{(E_{\pi^-} + E_{\pi^0})} \qquad \text{and} \qquad y^\tau_+ = \frac{(E_{\pi^+} - E_{\pi^0})}{(E_{\pi^+} + E_{\pi^0})} \tag{15}$$

and selecting

$$y^\tau > 0 \qquad \text{or} \qquad y^\tau < 0 \quad , \qquad \text{where } y^\tau = y^\tau_- y^\tau_+ , \tag{16}$$

the events are divided into two classes. The resulting distributions are shown in Fig. 3 for the gluon-gluon fusion process $pp \to h \to \tau^-\tau^+ \to \rho^-\rho^+ + 2\nu$ for the LHC (13 TeV).
The definition of φ^*_{CP} in Eq. (14) has been chosen such that the resulting Higgs-boson distributions in Fig. 3 left, i.e. for $y^\tau > 0$, agree with the respective distribution obtained with the impact parameter method and with those[7] of Ref. [18]. For $y^\tau < 0$ (Fig. 3, right) all φ^*_{CP} distributions are shifted by $\varphi^*_{CP} \to \varphi^*_{CP} + \pi$, as compared to those of Fig. 3, left. This is because in this case the product of the two $\tau^\mp \to \rho^\mp$ spin-analyzing functions is negative.
The cuts on y^τ are academic because the τ rest frames can in general not be reconstructed. Therefore, we use in the following the variables

$$y^L_- = \frac{\left(E^L_{\pi^-} - E^L_{\pi^0}\right)}{\left(E^L_{\pi^-} + E^L_{\pi^0}\right)} \qquad \text{and} \qquad y^L_+ = \frac{\left(E^L_{\pi^+} - E^L_{\pi^0}\right)}{\left(E^L_{\pi^+} + E^L_{\pi^0}\right)} , \tag{17}$$

[7] The distributions given in [16, 17, 19, 20] are shifted by an angle of π due to a different definition of φ^* which uses normalized vectors perpendicular to the planes spanned by the ρ mesons and their decay products.

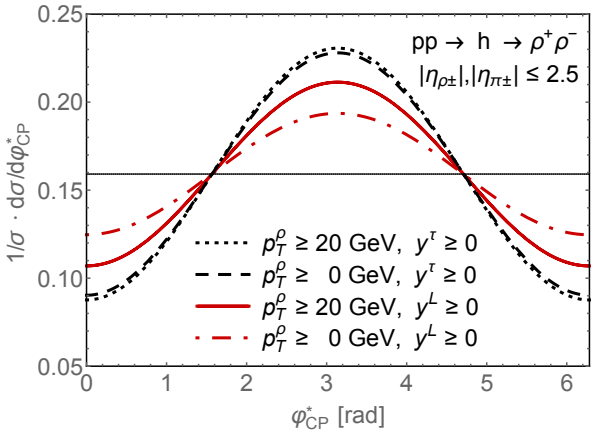

Figure 4. φ^*_{CP} distribution defined in Eq. (14) for $pp \to h \to \tau^-\tau^+ \to \rho^-\rho^+ + 2\nu$ at LHC (13 TeV) for a CP-even Higgs boson using the ρ-decay plane method. The black dotted and black dashed line (solid red line and dot-dashed red line) show the distribution if the cut on $y = y_1 y_2$ is performed in the corresponding τ rest frames (in the laboratory frame). For the distributions displayed by the solid red line and black dotted line an additional cut of $p_{T\rho} \geq 20$ GeV on the hadronic τ-jet was applied.

where $E^L_{\pi^\pm}$ and $E^L_{\pi^0}$ energies of the charged and the neutral pions associated with the decays of $\rho^\pm$ in the laboratory frame. Again, using $y^L = y^L_- y^L_+$ one separates events into two classes according to $y^L > 0$ and $y^L < 0$.

The effect of selecting events with respect to the sign of y^τ and y^L on the φ^*_{CP} distribution are compared in Fig. 4 for the case of a CP-even Higgs boson. If no cuts on the transverse momenta of the ρ mesons are applied the asymmetry (12) associated with the curve $y^L \geq 0$ (red dot-dashed line, $A^{\rho\rho} \simeq 14\%$) is reduced considerably with respect to the one for $y^\tau \geq 0$ (black dashed line, $A^{\rho\rho} \simeq 28\%$).

However, the situation is different if a minimum p_T-cut on the hadronic jet from $\tau \to \rho$ decay is imposed. We use $p_{T\rho} \geq 20$ GeV. At the LHC such a cut is indispensable in order to suppress the QCD background. In this case the asymmetry (12) is much less reduced if one selects the events with respect to y^L rather than y^τ, namely from $A^{\rho\rho} \simeq 29\%$ to $A^{\rho\rho} \simeq 21\%$.

C. Combination of impact parameter and ρ-decay plane method

In this section we combine the impact parameter and ρ-decay plane method of Sec. II A and II B and define the discriminating variable φ^*_{CP} for this case.

Let us consider the decay channels $h \to \tau^-\tau^+ \to a^-\rho^+$. For the $\tau^+ \to \rho^+ \to \pi^+\pi^0$ decay we assume that the momenta of the charged and neutral pion can be measured. The τ^- may decay via one of the major decay channels $\tau^- \to a^-$ listed in Eqs. (3) - (7), including the

decay via a ρ^- meson[8]. For the τ^- decay we demand a non-vanishing impact parameter of the final charged prong a^-.

As before, the variable φ^*_{CP} will be defined in the zero-momentum-frame of the final charged prongs $a^-a'^+$, where in the case at hand $a^- = e^-, \mu^-, \pi^-$ and $a'^+ = \pi^+$. The π^+ and π^0 momenta from $\tau^+ \to \rho^+$ decay are boosted into the $a^-a'^+$ ZMF and we calculate in this frame, as described in Sec. II B, the transverse neutral-pion direction with respect to the charged pion momentum. The resulting normalized vectors are denoted by $\hat{\mathbf{q}}^{*0+}_\perp$ and $\hat{\mathbf{q}}^{*+}$, respectively. For the $\tau^- \to a^-$ decay we boost the 4-momentum of the charged prong and its corresponding impact parameter vector $n^{\mu-} = (0, \hat{\mathbf{n}}^-)$ also into the $a^-a'^+$ ZMF. The resulting 4-vectors are denoted by $q^{\mu*-}$ and $n^{\mu*-}$. In the $a^-a'^+$ ZMF we calculate the normalized transverse vector $\hat{\mathbf{n}}^{*-}_\perp$ as described in in Sec. II A. The normalized 3-momentum of the charged prong a^- is denoted by $\hat{\mathbf{q}}^{*-}$. With these variables, an angle φ^* and a triple correlation $\mathscr{O}^*$ are defined by

$$\varphi^* \;=\; \arccos\left(\hat{\mathbf{q}}^{*0+}_\perp \cdot \hat{\mathbf{n}}^{*-}_\perp\right), \qquad\qquad \mathscr{O}^* \;=\; \hat{\mathbf{q}}^{*-} \cdot \left(\hat{\mathbf{q}}^{*0+}_\perp \times \hat{\mathbf{n}}^{*-}_\perp\right), \tag{18}$$

and the resulting variable which is sensitive to the CP nature of h is, as before,

$$\varphi^*_{CP} = \begin{cases} \varphi^* & \text{if } \mathscr{O}^* \geq 0 \\ 2\pi - \varphi^* & \text{if } \mathscr{O}^* < 0 \end{cases}, \qquad \text{with} \quad 0 \leq \varphi^*_{CP} \leq 2\pi\,. \tag{19}$$

In order to obtain a non-trivial φ^*_{CP} distribution one has to separate, as described in Sec. II B, events from $\tau^+ \to \rho^+$ decay which have positive and negative values of y^L_+ defined in (17). Also the $\tau^- \to a^-$ events may have to be divided into two classes, depending on the decay mode, cf. [13]. For the direct decay $\tau^- \to \pi^- + \nu_\tau$, for $\tau^- \to a_1^{-L,T} + \nu_\tau$, and for the leptonic decays $\tau^- \to l^- + \bar{\nu}_l + \nu_\tau$ such a separation is, however, not necessary.

For the decays $h \to \tau^-\tau^+ \to \rho^- a^+$ one proceeds analogously to the charge-conjugate modes described above. In this case the angle φ^* and $\mathscr{O}^*$ are defined by

$$\varphi^* \;=\; \arccos\left(\hat{\mathbf{q}}^{*0-}_\perp \cdot \hat{\mathbf{n}}^{*+}_\perp\right), \qquad\qquad \mathscr{O}^* \;=\; \hat{\mathbf{q}}^{*-} \cdot \left(\hat{\mathbf{n}}^{*+}_\perp \times \hat{\mathbf{q}}^{*0-}_\perp\right), \tag{20}$$

and φ^*_{CP} is given again by (19). Here , the events from $\tau^- \to \rho^-$ decay which have positive and negative values of y^L_- (cf. (17)) have to be separated. In addition, also the $\tau^+ \to a^+$ may have to be divided into two classes, see [13].

For the decays $h \to \tau^-\tau^+ \to a^-\rho^+$ the definition of the angle φ^*_{CP} is sketched in Fig. 5, left. For the specific case where τ^- decays directly to π^-, the φ^*_{CP} distribution is shown for events with $y^\tau_+ > 0$ in Fig. 5, right. For demonstration purposes we used here the variable $y^\tau_+ > 0$ defined in (15) rather than y^L_+. Cuts as given in the caption of this figure are applied. The

[8] Here we assume that the momenta of the charged and neutral pion from ρ^- decay can not be separated with sufficient precision. Otherwise one would use the ρ-decay plane method as described in Sec. II B.

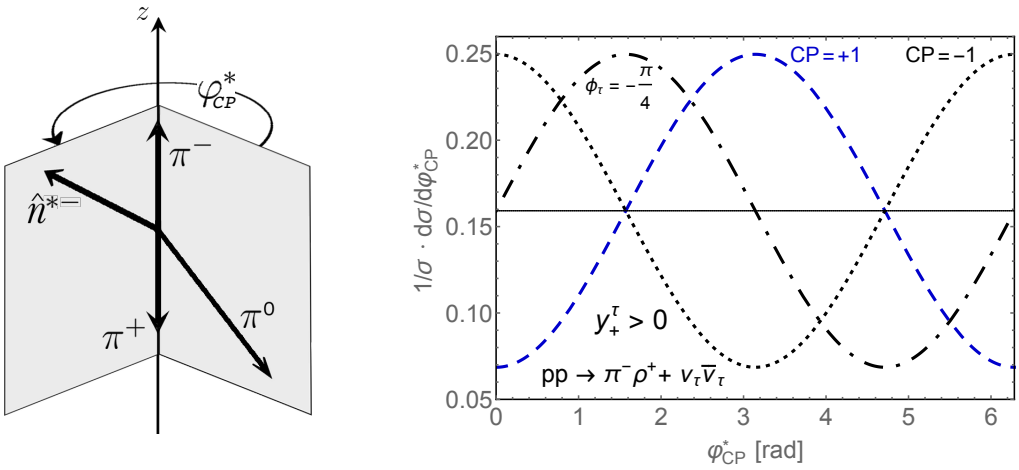

Figure 5. Left: Definition of the angle φ^*_{CP} in case of the combined method. Right: Normalized φ^*_{CP} distributions, Eq. (19), for $pp \to h \to \tau^-\tau^+ \to \pi^-\rho^+ + 2\nu_\tau$ events with $y^\tau_+ > 0$ at the LHC (13 TeV). The cuts $q^{\pi^-}_T, p^{\rho^+}_T \geq 20$ GeV and $|\eta_{\rho^+}|, |\eta_{\pi^\pm}| \leq 2.5$ were applied. The blue dashed, black dotted, and black long-dashed lines show the distribution for a *CP*-even Higgs boson ($\phi_\tau = 0$), a *CP*-odd Higgs boson ($\phi_\tau = \pm\pi/2$), and a *CP* mixture ($\phi_\tau = -\pi/4$), respectively. The flat line is the distribution due to Drell-Yan production. The distributions for events with $y^\tau_+ < 0$ are shifted by $\varphi^*_{CP} \to \varphi^*_{CP} + \pi$.

asymmetry (12) computed from these distributions is $A = 36\,\%$. This asymmetry is somewhat larger than the asymmetry associated with the decay $h \to \tau^-\tau^+ \to \rho^-\rho^+$ (cf. Fig. 3), because the τ-spin analyzing power of the direct decay $\tau^- \to \pi^-$ is one. The distributions for $y^\tau_+ < 0$, which are not shown, are shifted by $\varphi^*_{CP} \to \varphi^*_{CP} + \pi$.

The φ^*_{CP} distributions for the reactions with charge-conjugate final states, $pp \to h \to \tau^-\tau^+ \to \rho^-\pi^+ + 2\nu_\tau$, are the same as those shown in Fig. 5, right, for events with $y^\tau_- > 0$ and if cuts analogous to those given in the caption of this figure are applied. The distributions for events with $y^\tau_- < 0$ are again shifted by $\varphi^*_{CP} \to \varphi^*_{CP} + \pi$.

Let us consider, for definiteness, the decay of a CP-even Higgs boson. Fig. 6, left, shows the φ^*_{CP} distribution for $h \to \pi^-\rho^+$ obtained with the combined method (solid red line), while the dashed blue line is the distribution for $h \to \rho^-\rho^+$ obtained with the ρ-decay plane method. For $h \to \pi^-\rho^+$ the height of the distribution is somewhat larger than for $h \to \rho^-\rho^+$. This demonstrates the importance of using the combined method for eventually attaining a good precision of the Higgs mixing angle ϕ_τ. The φ^*_{CP} distribution (dot-dashed black line) for $h \to l^-\rho^+$ is also shown in this figure, This distribution has its minimum at $\varphi^*_{CP} = \pi$ because the τ-spin analyzing function of l^- is negative.

The plots in Fig. 6, right, demonstrate that a realistic event selection, i.e., applying the laboratory-frame cut $y^L_+ > 0$, does not significantly change the shape of the distribution. Because here only one ρ meson is involved, the effect of such a cut is much smaller than

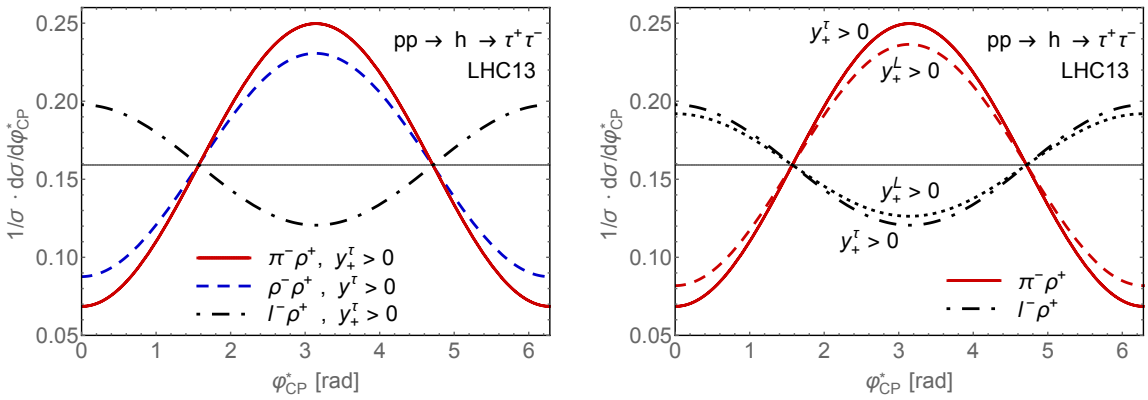

Figure 6. Normalized φ^*_{CP} distributions for a CP-even Higgs boson at the LHC (13 TeV). The cuts $p_T^{\rho^\pm} \geq 20$ GeV, $|\eta_{\rho^\pm}|, |\eta_{\pi^\pm}|, |\eta_{l^-}| \leq 2.5$ were applied. The dashed blue line (left plot) is the distribution for $h \to \rho^-\rho^+$, as in Fig. 3, left. The solid red and dashed red lines (left and right plot) correspond to $h \to \pi^-\rho^+$ with the additional cut $q_T^{\pi^-} \geq 20$ GeV. The dot-dashed black and dotted black lines (left and right plots) correspond to $h \to l^-\rho^+$ with the additional cut $q_T^{l^-} \geq 20$ GeV. The distributions shown in the left plot were computed with the cuts $y^\tau > 0$ and $y_+^\tau > 0$. The plot on the right shows the reduction of the height of the distributions if the laboratory-frame cut $y_+^L > 0$ is applied.

for $h \to \rho^+\rho^-$.

We have also investigated the impact of measurement uncertainties on the φ^*_{CP} distributions, both for the signal reactions and the Drell-Yan background. In Fig. 7 we show this impact for a CP-even Higgs boson and for the channels $\tau^-\tau^+ \to \pi^-\rho^+$ and $\tau^-\tau^+ \to l^-\rho^+$. We applied the cuts $p_T^{\rho^+} \geq 20$ GeV, $|\eta_{\rho^+}|, |\eta_{\pi^+}| \leq 2.5$ for $\tau^+ \to \rho^+$ and $q_T^{\pi^-,l^-} \geq 20$ GeV, $|\eta_{\pi^-}|, |\eta_{l^-}| \leq 2.5$ for $\tau^- \to \pi^-, l^-$. The experimental uncertainties are simulated with a Gaussian smearing of the impact parameter vectors of the charged tracks and the 4-momenta of the final electrons, muons, charged and neutral pions as described in [13]. For those τ decays where the impact parameter method is used to define φ^*_{CP}, the primary vertex (PV) is smeared using $\sigma_z^{PV} = 20\mu$m, $\sigma_{tr}^{PV} = 10\mu$m, $\sigma_{tr}^{a^\pm} = 10\mu$m, and the uncertainty on the intersection of the impact parameter vector and the charged tracks is simulated with $\sigma_{tr}^{\pi^-,l^-} = 10\mu$m. The charged pion and lepton momenta are smeared[9] using $\sigma_\theta^{a^\pm} = 1$ mrad and $\Delta E^{a^\pm}/E^{a^\pm} = 5\%$. For the pions from $\tau^\pm \to \rho^\pm$ decay we use for the charged pion momenta $\sigma_\theta^{\pi^\pm} = 1$ mrad, $\Delta E^{\pi^\pm}/E^{\pi^\pm} = 5\%$ and for the neutral pion momenta $\sigma_\theta^{\pi^0} = 0.025/\sqrt{12}$ rad [32], and $\Delta E^{\pi^0}/E^{\pi^0} = 10\%$.

As Fig. 7, left, shows, the impact of this smearing on the φ^*_{CP} distribution for the $\tau^-\tau^+ \to \pi^-\rho^+$ decay mode is rather small if only the uncertainty of the π^0 momentum is taken into account (dotted black line). The uncertainty is dominated by the angular resolution $\sigma_\theta^{\pi^0}$. The uncertainty of the $\pi^\pm$ momenta has a much larger effect on the distribution (dashed

[9] We consider a cone with opening angle θ around the particle track and σ_θ denotes the smearing parameter around the track.

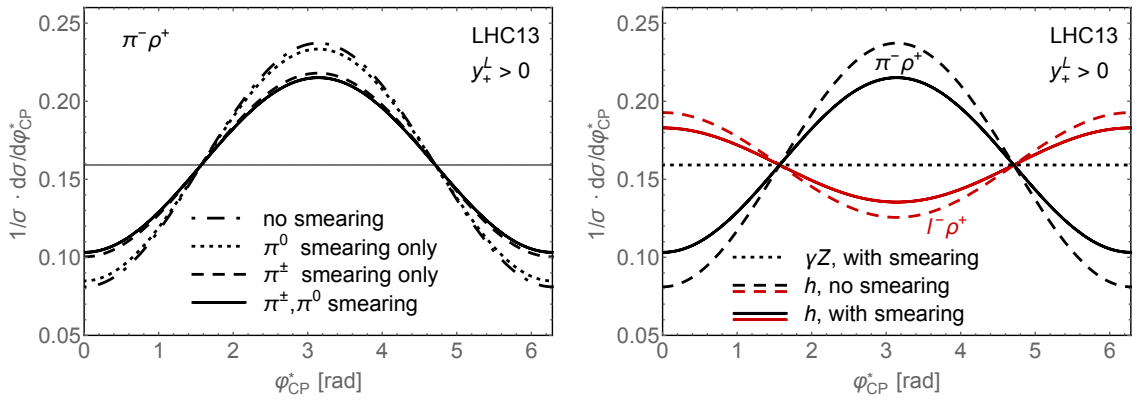

Figure 7. Impact of measurement uncertainties on φ^*_{CP} distributions. Left: CP-even Higgs boson $h \to \tau^-\tau^+ \to \pi^-\rho^+$. Right: signal (solid black and red lines) and background (black dotted line) distributions for $\pi^-\rho^+$ and $l^-\rho^+$ final states.

black line) and is dominated by the smearing of the π^- impact parameter caused by the uncertainties σ_z^{PV}, σ_{tr}^{PV}, and $\sigma_{tr}^{\pi^\pm}$. The solid black line shows the distribution taking into account all uncertainties.

In Fig. 7, right, we display the effect of the above smearing parameters on the distributions for the decays to $\pi^-\rho^+$ and $l^-\rho^+$, both for the signal and the Drell-Yan background. As shown in this figure the normalized φ^*_{CP} distribution of the Z^*/γ^* background is not affected by the smearing. This is in contrast to the case of the distributions for those $\tau^-\tau^+$ decay modes where for both τ decays the impact parameter method has to be used [13].

III. ESTIMATE OF THE EXPECTED PRECISION ON ϕ_τ

In this section we estimate the precision with which the mixing angle ϕ_τ may be determined for the $h(125\text{GeV})$ Higgs boson at the LHC (13 TeV) using the methods described in Sec. II A - II C. As in [13] we generate the φ^*_{CP} distributions for Higgs-boson production by gluon-gluon fusion and for the Drell-Yan background $Z^*/\gamma^* \to \tau^-\tau^+$ for all major τ-decay modes (3) - (7). We use the ρ-decay plane method of Sec. II B if both τ leptons decay to ρ mesons and the combined method of Sec. II C in case only one of the τ leptons decays to ρ. For all other τ-decay modes the impact parameter method is employed as described in Sec. II A.

In order to compute the asymmetries (12) for the different decay channels, we apply the following experimentally motivated cuts: We require the τ-pair invariant mass $M_{\tau\tau} \geq 100$ GeV for all $\tau^-\tau^+$ decay channels. For the decays $\tau^\pm \to \rho^\pm + \nu \to \pi^\pm + \pi^0 + \nu$, we demand $p_T^{\rho^\pm} \geq 20$ GeV and $|\eta_{\rho^\pm}|, |\eta_{\pi^\pm}| \leq 2.5$. For the decays $\tau^\pm \to l^\pm + 2\nu$ and $\tau^\pm \to \pi^\pm + \nu$ we

$\tau\tau$ decay channel	A_S [%]	$\frac{S}{S+B}$	A_{S+B} [%]
hadron-hadron	16.2	0.5	8.1
lepton-hadron	9.4	0.5	4.7
lepton-lepton	4.5	1/3	1.5

Table I. LHC13; Asymmetries for the hadron-hadron, lepton-hadron, and lepton-lepton decay modes, obtained with the set of cuts and smearing parameters described in the text.

apply the cuts $q_T^{\pi^\pm,l^\pm} \geq 20$ GeV and $|\eta_{\pi^\pm}|, |\eta_{l^\pm}| \leq 2.5$. Furthermore, we assume that the longitudinal and transverse helicity states $a_1^{L,T\pm}$ of the a_1 resonance can be reconstructed and we use the cuts $p_T^{a_1^\lambda} \geq 20$ GeV and $|\eta_{a_1^\lambda}| \leq 2.5$ for the decays $\tau^\pm \to a_1^{L,T\pm} + \nu$.
The experimental uncertainties are simulated by performing a Gaussian smearing of the 4-momenta and impact parameter vectors as described in Sec. II C.
The asymmetries for those $h \to \tau^+\tau^-$ decay channels, where at least one τ lepton decays to a ρ meson, can be directly calculated from the smeared φ^*_{CP} distributions of the signal reactions, because the respective φ^*_{CP} distribution of the Drell-Yan background is flat, cf. Sec. II C. For those channels, where the impact parameter method has to be used both for the τ^- and τ^+ decay, the shapes of the signal and background φ^*_{CP} distribution are deformed due to the smearing of the primary vertex. In these cases smeared asymmetries for the Higgs signal are computed as described in [13].
The resulting asymmetries of the signal distributions for the hadron-hadron, lepton-hadron, and lepton-lepton final states are given in the second column of Table I. The third column of Table I contains $S/(S+B)$ ratios taken from [33] which we use here. For the hadron-hadron and lepton-hadron decay channels we assume the ratio $S/B = 1$ and $S+B = 2\,\text{events/fb}$, while for the lepton-lepton decay modes we use $S/B = 1/2$ and $S+B = 2\,\text{events/fb}$. With these numbers, we obtain the asymmetries $A_{S+B} = A_S \times S/(S+B)$ given in column 4 of Table I.
With A_{S+B} and the expected total number of events we estimate with a procedure described in [13] the error $\Delta\phi_\tau$ with which the mixing angle ϕ_τ can be determined at the LHC. We obtain that ϕ_τ can be measured with an uncertainty of 15° (9°) if an integrated luminosity of $150\,\text{fb}^{-1}$ ($500\,\text{fb}^{-1}$) will be collected. If eventually a luminosity of $3\,\text{ab}^{-1}$ could be achieved, the precision on ϕ_τ may reach 3.6°. The hadron-hadron decay modes of the $\tau^+\tau^-$ pair yield the highest precision: for instance, assuming an integrated luminosity of $3\,\text{ab}^{-1}$ we obtain $\Delta\phi_\tau \simeq 4°$ for these modes, while the hadron-lepton and lepton-lepton decay channels yield $\Delta\phi_\tau \simeq 7°$ and $\Delta\phi_\tau \simeq 22°$, respectively. These results show that using both the impact parameter and the ρ-decay plane method and their combination improves the precision on ϕ_τ compared with the achievable precision using only the impact parameter method. With this method we obtained in [13] for the combination of all decay channels the estimates $\Delta\phi_\tau \simeq 27°$ ($150\,\text{fb}^{-1}$),

$\Delta\phi_\tau \simeq 14^\circ$ ($500\,\mathrm{fb}^{-1}$), and $\Delta\phi_\tau \simeq 5^\circ$ ($3\,\mathrm{ab}^{-1}$).
It should be noted that the above estimates depend on the Higgs-boson production process and, in particular, on the transverse momentum of the Higgs boson. For Higgs-boson events with large large transverse momenta, the asymmetries decrease somewhat compared to the numbers given in Table I. In addition, the achievable precision on ϕ_τ strongly depends on the experimental resolution of the measurement of the impact parameters and on the angular resolution of the determination of the π^0 tracks.

IV. IMPACT ON TWO-HIGGS-DOUBLET MODELS

In this section we analyze the impact of future measurements of the Higgs mixing angle ϕ_τ and of the reduced τ-Yukawa coupling strength κ_τ on several SM extensions with a non-standard Higgs sector.
Neutral Higgs bosons with CP-violating couplings to quarks and leptons appear in many SM extensions in a natural way. Here, we restrict ourselves to non-supersymmetric SM extensions. (For recent discussions of Higgs-sector CP violation in the context of supersymmetry, see [34–36].)
Two-Higgs-doublet models (2HDM) are among the simplest SM extensions which allow for a reduced Yukawa coupling strength $\kappa_\tau \neq 1$ and/or a mixing angle $\sin\phi_\tau \neq 0$ in the interactions of the 125 GeV Higgs resonance with τ leptons as parametrized by (2). These models are based on the SM gauge group and the SM field content is extended by an additional Higgs doublet. The physical particle spectrum of these models contains three neutral Higgs particles h_i $(i = 1,2,3)$, one of which is to be identified with the 125 GeV resonance, and a charged Higgs boson and its antiparticle, $H^\pm$. CP-violating Yukawa couplings of neutral Higgs bosons to quarks and leptons, in particular to τ leptons, appear in these models in a natural way. (For a recent review of these models, see, for instance, [37].)
In the following we discuss the implications of future measurements of the reduced Yukawa coupling strength κ_τ and of the mixing angle ϕ_τ on the parameter spaces of several variants of 2HDM. As estimated in Sec. III, we assume that ϕ_τ can be measured during the high-luminosity run of the LHC (13 TeV) with a precision of $\Delta\phi_\tau = \pm 9^\circ$ and eventually [10] $\pm 4^\circ$. For κ_τ a precision of $\pm 4\,\%$ can be expected [38].
Let us first translate these expected experimental precisions into bounds on the reduced Yukawa couplings to $\tau^-\tau^+$ of the 125 GeV resonance. In the following, we denote the 125 GeV Higgs boson by h_1. Additional neutral Higgs bosons may exist – we assume here and in the following that they are non-degenerate with h_1. The flavor-conserving Yukawa

[10] This precision could also be achieved at a future high-luminosity e^+e^- collider, cf. [15].

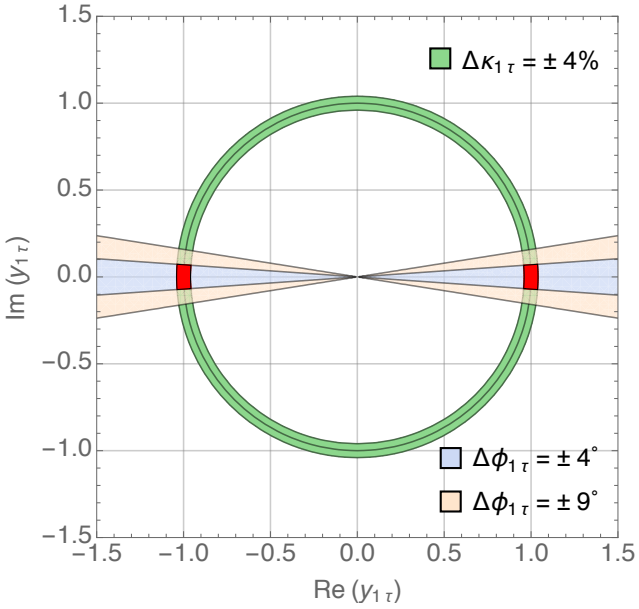

Figure 8. Allowed regions in the space of the reduced τ-Yukawa couplings $\mathrm{Re}(y_{1\tau})$, $\mathrm{Im}(y_{1\tau})$ for assumed measurements of $\kappa_{1\tau} = 1.0 \pm 0.04$ and $\phi_{1\tau} = 0^\circ \pm 9^\circ$ (grey segments) and $\phi_{1\tau} = 0^\circ \pm 4^\circ$ (red segments), respectively.

interactions of neutral Higgs bosons h_i to quarks and leptons $f = q, l$ may be parametrized in a model-independent way as follows:

$$\mathscr{L}_Y = -\frac{m_f}{\mathrm{v}} \left(\mathrm{Re}(y_{if})\ \bar{f} f + \mathrm{Im}(y_{if})\ \bar{f} i\gamma_5 f \right) h_i \,, \tag{21}$$

where a sum over f and i is understood. We concentrate here on the reduced τ Yukawa couplings $\mathrm{Re}(y_{1\tau})$ and $\mathrm{Im}(y_{1\tau})$. Assuming that future measurements yield[11] $\kappa_{1\tau} = 1.0 \pm 0.04$ and $\phi_{1\tau} = 0^\circ \pm 9^\circ$, respectively $\phi_{1\tau} = 0^\circ \pm 4^\circ$, one gets the very small areas displayed in Fig. 8 within which $\mathrm{Re}(y_{1\tau})$ and $\mathrm{Im}(y_{1\tau})$ must lie. Notice that only the relative sign $\mathrm{Re}(y_{1\tau})$ and $\mathrm{Im}(y_{1\tau})$ is fixed, because the measured value of $\phi_{1\tau}$ cannot be distinguished from $\phi_{1\tau} + \pi$.

A. The aligned 2HDM

Phenomenologically viable 2HDM are usually constructed such that flavor-changing neutral current (FCNC) interactions are absent at tree level. This may be achieved by requiring Yukawa couplings such that none of the right-chiral quark and lepton fields f_R couples to both Higgs doublets Φ_1, Φ_2. It can be enforced by assuming an appropriately chosen discrete Z_2 symmetry (which is exactly obeyed by the Yukawa Lagrangian), and there are several possible implementations of such a symmetry (cf., for instance, [37]). (Below we shall call these

[11] In this section we put an additional label on κ_τ and ϕ_τ referring to the Higgs boson h_i.

models 'conventional 2HDM'.) Tree-level flavor conservation of the neutral Higgs interactions can also be enforced by allowing both Higgs doublets to couple to f_R but assuming that the Yukawa coupling matrices of Φ_1 and Φ_2 are aligned in flavor space. While this is also an ad hoc assumption, it is attractive from the phenomenological point of view: the resulting model, the so-called aligned two-Higgs doublet model (A2HDM) formulated in [21] contains as special cases all known 2HDM with tree-level neutral-current flavor conservation, and it contains possible new sources of CP violation. Apart from CP-violating mixing of the neutral Higgs-boson states caused by a Higgs potential which is CP-violating already at tree level, each of the aligned Yukawa matrices of the u-, d-type quark and charged lepton sector may contain a CP phase which affects the Yukawa couplings of the neutral Higgs bosons and those of the charged Higgs boson.

The general gauge-invariant, hermitean, and renormalizable Higgs potential $V(\Phi_1,\Phi_2)$ of 2HDM, which applies also to the A2HDM, breaks the CP symmetry if no restriction on the parameters of V is imposed. CP violation by V is caused by complex couplings of soft and hard Z_2-symmetry breaking terms in V. If this is the case, the physical CP-even and -odd neutral Higgs fields mix and the neutral fields respectively states h_1,h_2,h_3 in the mass basis are CP mixtures already at tree level. In the context of the A2HDM we use, as Ref. [21], the Higgs doublets Φ_1, Φ_2 in the so-called Higgs basis, where only Φ_1 has a non-zero vacuum expectation value. In this basis, the doublets can be brought into the form

$$\Phi_1 = \left(G^+, (\mathrm{v}+S_1+iG^0)/\sqrt{2}\right)^T, \qquad \Phi_2 = \left(H^+, (S_2+iS_3)/\sqrt{2}\right)^T, \tag{22}$$

where G^+ and G^0 are the Goldstone fields, H^+ is the physical charged Higgs-boson field, and S_1, S_2 and S_3 are the physical neutral fields, which are CP-even and -odd, respectively. They are related to the fields h_1,h_2,h_3 in the mass basis by

$$(h_1,h_2,h_3)^T = R(S_1,S_2,S_3)^T, \tag{23}$$

where R is a real orthogonal 3×3 matrix. The matrix elements of R depend on the parameters of the potential. Using (23), the Yukawa interactions (21) of the h_i to quarks and leptons, i.e., the reduced Yukawa couplings to d-type quarks, charged leptons l, and u-type quarks are given by [21]:

$$y_{id,l} = R_{i1} + (R_{i2}+iR_{i3})\zeta_{d,l}, \tag{24}$$

$$y_{iu} = R_{i1} + (R_{i2}-iR_{i3})\zeta_u^*, \tag{25}$$

where the complex parameters ζ_u,ζ_d,ζ_l appear in the alignment ansatz for the Yukawa matrices [21] and provide additional sources of CP violation. The Yukawa interactions of the charged Higgs bosons $H^\pm$, which involve also these complex parameters and the Cabibbo-Kobayashi-Maskawa quark mixing matrix, are not needed in the following.

The general reduced Yukawa couplings (24), (25) contain a number of unknown parameters: three mixing angles which parametrize R and the three complex parameters $\zeta_u, \zeta_d, \zeta_l$. We may identify the 125 GeV Higgs resonance with h_1 (see below). The allowed regions of the reduced Yukawa couplings of h_1 to τ leptons, $\mathrm{Re}(y^i_{1\tau})$ and $\mathrm{Im}(y_{1\tau})$, which depend on five unknown parameters, are those displayed in Fig. 8 if the envisaged experimental precisions can be attained. The determination of the unknown parameters which determine the Yukawa couplings (24), (25) of the A2HDM requires a global fit, with the (future) measurements of $\kappa_{1\tau}$ and $\phi_{1\tau}$ being part of the input, which is beyond the scope of this paper. We consider here two special cases which are also of relevance for our purpose, namely the A2HDM with complex parameter ζ_l and a Higgs potential that is CP-conserving at tree-level and the model with Higgs-sector CP violation and real ζ_l. We discuss constraints on the parameters of these models resulting solely from measurements of $\kappa_{1\tau}$ and $\phi_{1\tau}$.

1. Tree-level CP-conserving Higgs potential and complex ζ_l:

In this case there is no mixing of S_3 with S_1, S_2 at tree level. The 3×3 matrix R is now block-diagonal, with $R_{13} = R_{23} = R_{31} = R_{32} = 0$ and $R_{33} = 1$. The mass eigenstates h_1 and h_2, which result from the mixing of S_1 and S_2, are CP-even and $h_3 = S_3$ is CP-odd. (The assignment of the CP quantum numbers to these states is determined by their tree-level couplings to the weak gauge bosons.) Because the LHC results [3, 4] exclude that the 125 GeV Higgs resonance is a pseudoscalar (which has no tree-level couplings to W^+W^- and ZZ), it cannot be identified with h_3. By convention we may identify it with h_1. The reduced τ-Yukawa couplings are in this case:

$$\mathrm{Re}(y_{i\tau}) = R_{i1} + R_{i2}\,\mathrm{Re}(\zeta_l)\,, \quad \mathrm{Im}(y_{i\tau}) = R_{i2}\,\mathrm{Im}(\zeta_l)\,, \quad i = 1,2\,, \tag{26}$$

$$\mathrm{Re}(y_{3\tau}) = -\mathrm{Im}(\zeta_l)\,, \qquad \mathrm{Im}(y_{3\tau}) = \mathrm{Re}(\zeta_l)\,. \tag{27}$$

These equations show that the Higgs bosons h_i can couple already at tree level to both scalar and pseudoscalar τ lepton currents, due to the additional CP violation provided by the complex parameter ζ_l from the aligned Yukawa sector, although the h_i are CP eigenstates at tree level with respect to their interactions with weak gauge bosons. Thus, also in this special case of the A2DHM a nonzero value of $\sin\phi_{1\tau}$ is possible. One should however notice that the CP-violating Yukawa couplings (26), (27) induce at the 1-loop level CP-violating terms in the effective Higgs potential which in turn lead to CP-violating mixing of the h_i at the loop level. Therefore, beyond the tree level, the h_i are no longer CP eigenstates.
The 2×2 orthogonal submatrix (R_{ij}) $(i,j = 1,2)$ depends on one parameter; i.e., for fixed i, the two equations (26) depend on three unknowns. Thus, in order to determine these parameters, further experimental input is needed, apart from the measurement of the reduced

coupling strength $\kappa_{1\tau}$ and of $\phi_{1\tau}$. Suppose this input implies that $R_{12} \neq 0$. From Eq. (26) one gets for $i = 1$, using the orthogonality of R and $|\mathrm{Im}(y_{1\tau})/\mathrm{Im}(\zeta_l)| \leq 1$:

$$0 = \kappa_{1\tau}\left(\mathrm{Im}(\zeta_l)\cos\phi_{1\tau} - \mathrm{Re}(\zeta_l)\sin\phi_{1\tau}\right) \pm \mathrm{Im}(\zeta_l)\sqrt{1-\left(\kappa_{1\tau}\sin\phi_{1\tau}/\mathrm{Im}(\zeta_l)\right)^2}\,. \quad (28)$$

If it would turn out that $\kappa_{1\tau} = 1$, which corresponds to $\mathrm{Re}(y_{1\tau}) = 1$ and $\mathrm{Im}(y_{1\tau}) = 0$, Eq. (28) is fulfilled for all ζ_l. In this case one could restrict the parameters $\mathrm{Re}(\zeta_l), \mathrm{Im}(\zeta_l)$ using Eq. (26) if R_{12} is known from some other measurement, and if it is non-zero which is likely.

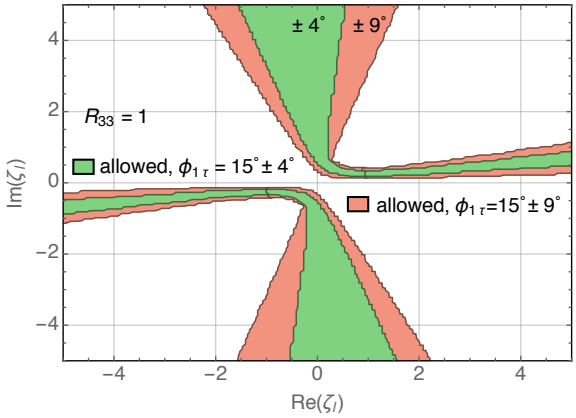

Figure 9. Aligned 2HDM with CP-conserving Higgs potential but $\mathrm{Im}(\zeta_l) \neq 0$. For illustration we assume $\phi_{1\tau}$ is measured with a central value of $\phi_{1\tau} = 15°$. The plot shows the resulting allowed areas to which the parameters $\mathrm{Re}(\zeta_l), \mathrm{Im}(\zeta_l)$are restricted if $\Delta\phi_{1\tau} = \pm 9°$ (red areas) and $\Delta\phi_{1\tau} = \pm 4°$ (green areas).

However, if a non-zero value of $\phi_{1\tau}$, e.g. $\phi_{1\tau} = 15° \pm 4°$ will be measured, the allowed parameter range of $\mathrm{Re}(\zeta_l)$ and $\mathrm{Im}(\zeta_l)$ can be restricted without knowing R_{12}, see Fig. 9. If $\phi_{1\tau}$ can be measured with a precision of 9° (4°), the red (green) areas in Fig. 9 display the ranges in which the parameters $\mathrm{Re}(\zeta_l)$ and $\mathrm{Im}(\zeta_l)$ must then lie. Fig. 9 is symmetric under a reflection at $\{\mathrm{Re}(\zeta_l), \mathrm{Im}(\zeta_l)\} = \{0,0\}$ which corresponds to the sign choice in $R_{11} = \pm\sqrt{1-R_{12}^2}$. Because $\phi_{1\tau}$ can be measured only modulo π, only the relative sign of $\mathrm{Re}(\zeta_l)$ and $\mathrm{Im}(\zeta_l)$ is fixed.

Existing experimental upper bounds on the electric dipole moments of the neutron and of atoms/molecules provide upper bounds on $|\mathrm{Im}(\zeta_u^*\zeta_d)|$ and $|\mathrm{Im}(\zeta_q^*\zeta_l|$, which depend, however, on the masses of the neutral and charged Higgs bosons [39].

2. *CP-violating Higgs potential and real ζ_l:*

Another limiting case of the A2HDM, which is also relevant for CP violation in the τ decays of the 125 GeV resonance, is the model with CP-violating tree-level Higgs potential but real

alignment parameters $\zeta_u, \zeta_d, \zeta_l$. In this case the reduced Yukawa couplings of the h_i read:

$$\mathrm{Re}(y_{id,l}) = R_{i1} + R_{i2}\zeta_{d,l}\,, \qquad \mathrm{Im}(y_{id,l}) = R_{i3}\zeta_{d,l}\,, \tag{29}$$

$$\mathrm{Re}(y_{iu}) = R_{i1} + R_{i2}\zeta_{u}\,, \qquad \mathrm{Im}(y_{iu}) = -R_{i3}\zeta_{u}\,. \tag{30}$$

The couplings (29) and (30) depend on six real parameters. We assume that $\kappa_{1\tau}$ and $\phi_{1\tau}$ will be measured with the precision as stated in the preceding subsection. For $\zeta_l \neq 0$, Eqs. (29) imply

$$0 \;=\; \kappa_{1\tau}\,(R_{12}\sin\phi_{1\tau} - R_{13}\cos\phi_{1\tau}) \;\pm\; R_{13}\sqrt{1-R_{12}^2-R_{13}^2}\,. \tag{31}$$

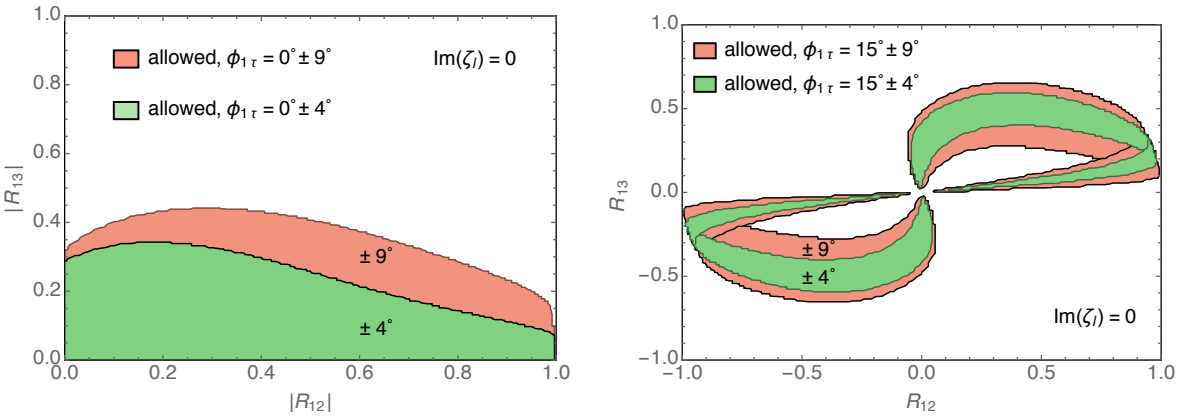

Figure 10. A2HDM with CP-violating Higgs potential and $\mathrm{Im}(\zeta_l) = 0$. Constraints on the mixing matrix elements R_{12} and R_{13} assuming that measurements yield $\phi_{1\tau} = 0^\circ$ (left plot) or $\phi_{1\tau} = 15^\circ$ (right plot). The red (green) areas show the allowed regions which would remain if $\phi_{1\tau}$ will be measured with a precision of $\Delta\phi_{1\tau} = \pm 9^\circ$ ($\Delta\phi_{1\tau} = \pm 4^\circ$). Notice that in the right plot the allowed regions are restricted to $|R_{12}| < 1$.

Relation (31) leads to constraints on the Higgs mixing matrix elements R_{12} and R_{13} which are illustrated in the left and right plot in Fig. 10. We recall that $\phi_{1\tau}$ will be experimentally determined with our method only modulo π. Thus, if the central value of $\phi_{1\tau}$ turns out to be zero, only the moduli R_{12} and R_{13} are constrained by (31). If $\phi_{1\tau}$ turns out to be non-zero, the relative sign of R_{12} and R_{13} is fixed by (31).

The mixing matrix elements R_{12} and R_{13} are restricted already by measurements of *CP*-even observables [40] and by existing upper bounds on electric dipole of the neutron and of atoms/molecules [39]. These constraints in the $R_{12} - R_{13}$ plane are different from those illustrated in Fig. 10. Thus, the measurement of $\phi_{1\tau}$ would, if interpreted within this model, either be evidence for Higgs-sector CP violation or further constrain this scenario.

B. Conventional 2HDM with neutral flavor conservation

As shown in [21] the aligned 2HDM contains as special cases the known 'conventional' 2HDM with tree-level neutral flavor conservation based on (approximate) Z_2 symmetries. We briefly discuss the implications of future measurements of $\kappa_{1\tau}$ and $\phi_{1\tau}$ on the parameters of these models.

1. Type-I and type-II model:

In the 2HDM of type-I, only the doublet ϕ_2 is coupled to fermions, while in the model of type-II, Φ_1 is coupled to d_R, l_R and Φ_2 is coupled to u_R. In these models no additional CP violation besides the Kobayashi-Maskawa phase arises from the Yukawa matrices. The parameters $\zeta_u, \zeta_d, \zeta_l$, which are real in these models, are no longer independent, but are given [21] in terms of the parameter $\beta = \arctan(\mathrm{v}_2/\mathrm{v}_1)$, where v_1 and v_2 are the vacuum expectations of the neutral components of the doublets Φ_1 and Φ_2, respectively. Thus, CP-violating effects caused by the Yukawa couplings of the neutral Higgs bosons h_i require for both models (and also for other conventional 2HDM) mixing of CP-even and-odd neutral states caused by a CP-violating Higgs potential. In this context it is customary to start from the usual representation of the doublets, $\Phi_j = (\varphi_j^+, (\mathrm{v}_j + \varphi_j + i\chi_j)/\sqrt{2})^T$, $(j = 1,2)$, and diagonalize the 3×3 squared mass matrix of the physical neutral Higgs bosons in the basis φ_1, φ_2, A, where $A = -\sin\beta\,\chi_1 + \cos\beta\,\chi_2$. This diagonalization is accomplished by an orthogonal matrix O. The neutral Higgs fields h_i in the mass basis are given by

$$(h_1, h_2, h_3)^T = O(\varphi_1, \varphi_2, A)^T\,. \tag{32}$$

The matrix O is related to the matrix R defined in (23) by

$$O = R \begin{pmatrix} \cos\beta & \sin\beta & 0 \\ -\sin\beta & \cos\beta & 0 \\ 0 & 0 & 1 \end{pmatrix}. \tag{33}$$

For the type-I and type-II 2HDM with neutral Higgs sector CP violation the reduced scalar and pseudoscalar Yukawa couplings (21) of the neutral Higgs bosons h_i are given in terms of the matrix elements of O as listed in Table II, cf. [41, 42].

In the type-I and -II 2HDM the neutral Higgs Yukawa couplings depend on 4 real parameters: three angles with which the matrix O can be parametrized, and $\tan\beta$. Other couplings of the h_i and of $H^\pm$ also depend on (some of) these parameters. Constraints from B physics and $B_0 - \bar{B}_0$ mixing imply that $\tan\beta$ should be larger than $0.5 - 0.7$ [43]. Recently a number of investigations were made within type-I and -II 2HDM with neutral Higgs sector CP violation,

Table II. Reduced Yukawa couplings (21) to quarks and leptons of the neutral Higgs bosons h_i in the type-I and type-II 2HDM.

	$\mathrm{Re}(y_{iu})$	$\mathrm{Re}(y_{id}) = \mathrm{Re}(y_{il})$	$\mathrm{Im}(y_{iu})$	$\mathrm{Im}(y_{id}) = \mathrm{Im}(y_{il})$
Type-I	$O_{i2}/\sin\beta$	$O_{i2}/\sin\beta$	$-O_{i3}\cot\beta$	$O_{i3}\cot\beta$
Type-II	$O_{i2}/\sin\beta$	$O_{i1}/\cos\beta$	$-O_{i3}\cot\beta$	$-O_{i3}\tan\beta$

including [44–50], on how LHC and B physics data and the present upper limits on the electric dipole moments of the neutron [51] and of the electron [52] constrain the mixing angles of O. In the following we employ the parametrization of O in terms of three angles, α, α_c, and α_b in the convention used in [48, 50]. In the CP-conserving limit of the type-I and -II 2HDM $\alpha_c = \alpha_b = 0$. The bounds on the CP angles α_c, α_b derived in [48, 50] depend, in particular, on the masses of the h_i and H^+. A measurement of the mixing angle $\phi_{1\tau}$ with some precision in the τ decays of the 125 GeV Higgs resonance would yield significant information on neutral Higgs-sector CP violation in the context of these models – independent of the masses of the charged and the other neutral Higgs bosons.

This can be seen as follows. We identify the 125 GeV Higgs with h_1. (The following argumentation can also be applied to the other neutral Higgs bosons.) For the Yukawa couplings of h_1 the matrix elements O_{1j} are relevant. Using the parametrization of O as in [48, 50], we have $O_{11} = -\sin\alpha\cos\alpha_b$, $O_{12} = \cos\alpha\cos\alpha_b$, $O_{13} = \sin\alpha_b$. That is, these matrix elements do not depend on α_c. Using that $\tan\phi_{1\tau} = \mathrm{Im}(y_{1l})/\mathrm{Re}(y_{1l})$ and $\kappa_{1,\tau} = [(\mathrm{Re}(y_{1l}))^2 + (\mathrm{Im}(y_{1l}))^2]^{1/2}$, and using the reduced Yukawa couplings of Table II, we get for

$$\text{Type I}: \qquad \tan\alpha_b = \frac{\cos\alpha}{\cos\beta}\,\tan\phi_{1\tau}\,, \tag{34}$$

$$\sin\alpha_b = \kappa_{1\tau}\tan\beta\;\sin\phi_{1\tau}\,, \tag{35}$$

$$\text{Type II}: \qquad \tan\alpha_b = \frac{\sin\alpha}{\sin\beta}\,\tan\phi_{1\tau}\,, \tag{36}$$

$$\sin\alpha_b = -\kappa_{1\tau}\cot\beta\;\sin\phi_{1\tau}\,. \tag{37}$$

Let's assume that future measurements would yield $\phi_{1\tau} = 0^\circ \pm 4^\circ$ and $\kappa_{1\tau} = 1 \pm 0.04$. The resulting constraints on the two-dimensional $\{|\sin\alpha_b|, \tan\beta\}$ parameter space of the type-I and type-II 2HDM are shown in Fig. 11, left and right, respectively. The white (colored) areas in Fig. 11, which depend on the assumptions on $\cos(\beta-\alpha)$ stated in the caption of the figure, are the remaining allowed (excluded) regions. The area above the solid red line would be excluded, independent of the values of the mixing angle α.

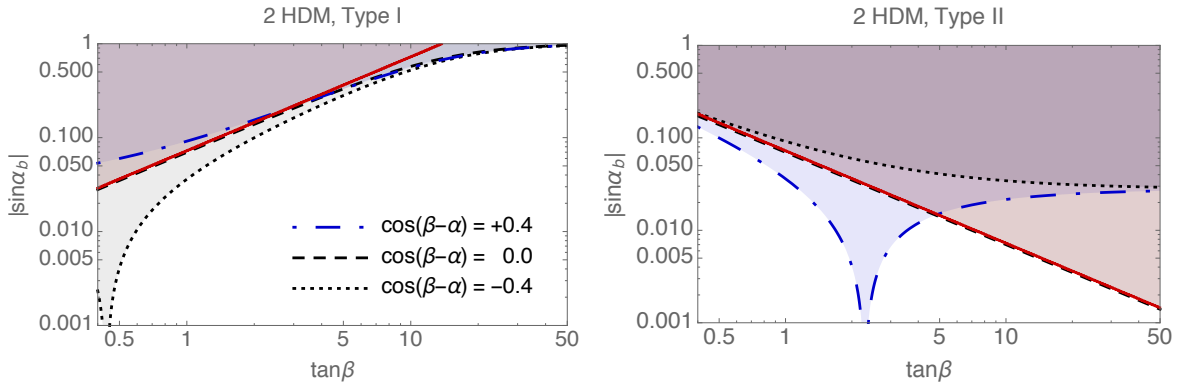

Figure 11. Exclusion ranges (colored) in the $|\sin\alpha_b|$, $\tan\beta$ parameter space, assuming that measurements yield $\phi_{1\tau} = 0^\circ \pm 4^\circ$. The area between the solid red lines and the top of the plots will then be excluded, irrespective of the value of the mixing angle α. The dot-dashed blue, dashed black, and dotted black lines are the boundaries of α-dependent exclusion ranges for fixed values of $\cos(\beta-\alpha) = 0.4, 0,$ and -0.4, respectively. Left: type I model; right: type II model.

Constraints on $\sin\alpha_b$ and $\tan\beta$ were derived in [50] using LHC results on h_1, on searches for $h_{2,3}$, and the experimental upper bounds on the EDM of the neutron and the electron. In some regions the constraints that will be obtainable solely from the measurement of $\phi_{1\tau}$ and $\kappa_{1\tau}$ are complementary to the constraints derived in [50]. In the region around $\tan\beta \sim 1$ the determination of $\phi_{1\tau}$ would actually provide a stronger constraint. One should also recall that the measurement of $\phi_{1\tau}$ probes Higgs-sector CP violation directly, while EDM of leptons and hadrons can be induced also by other non-standard CP-violating interactions.

2. *Flipped, lepton-specific, and inert model:*

The flipped 2HDM is defined by the coupling prescriptions $d_R \leftrightarrow \Phi_1$ and $u_R, l_R \leftrightarrow \Phi_2$, while the lepton-specific model is defined by $l_R \leftrightarrow \Phi_1$ and $u_R, d_R \leftrightarrow \Phi_2$. Overviews on the phenomenology of these models are given in [37, 53]. In the flipped 2HDM the Yukawa couplings of the h_i to u-type quarks and charged leptons are identical to the corresponding ones of the type-I model, while the Yukawa couplings to d-type quarks are those of type-II. In the lepton-specific model, the Yukawa couplings of the h_i to quarks are those of the type-I model, while the Yukawa couplings to charged leptons are those of type-II. Therefore, our discussion in the previous subsection of how future measurements of $\kappa_{1\tau}$ and $\phi_{1\tau}$ will provide information on the CP-violating Higgs-mixing parameter $|\sin\alpha_b|$ within the type-I and type-II models can be taken over. The left plot and right plot in Fig. 11 applies also to the flipped and lepton-specific 2HDM, respectively. In these models, the branching ratio of $h_1 \to \tau^+\tau^-$

can be larger than that of $h_1 \to b\bar{b}$, contrary to the case of type-I and type-II models.
Finally, a remark on the so-called inert model, which is a 2HDM with an unbroken Z_2 symmetry [37]. The Higgs-boson spectrum of this model contains a neutral state which is stable and will therefore contribute to the dark matter density. In this model, the tree-level Higgs potential is CP-invariant by virtue of the imposed Z_2 symmetry. Thus the inert 2HDM predicts $\sin\phi_{1\tau} = 0$ in $h_1 \to \tau^+\tau^-$.

V. CONCLUSIONS

We have investigated the precision with which the CP nature of the 125 GeV Higgs boson h can be determined in its decays to $\tau^-\tau^+$ at the LHC (13 TeV). We have taken into account all major τ-decays to charged prongs. Contrary to [13] where the impact parameter method was used for all τ decays in order to define an observable φ^*_{CP} which is sensitive to possible scalar-pseudoscalar Higgs mixing parametrized by an angle ϕ_τ, we combined in this paper two methods: We used the ρ-decay plane method for $\tau^\mp \to \rho^\mp$ and the impact parameter method for all other major τ decays. This combination leads to an increase of the sensitivity of φ^*_{CP} to the mixing angle ϕ_τ. In estimating this sensitivity we took into account the contributions from the Drell-Yan background, and we have analyzed by Monte-Carlo simulation how measurement uncertainties affect the signal and background φ^*_{CP} distributions. We found that the mixing angle ϕ_τ can be determined with an uncertainty of $\Delta\phi_\tau \simeq 15^\circ$ (9°) at the LHC with an integrated luminosity of $150\,\text{fb}^{-1}$ ($500\,\text{fb}^{-1}$). At the high-luminosity LHC with an integrated luminosity of $3\,\text{ab}^{-1}$ a precision of $\approx 4^\circ$ on ϕ_τ could be reached.
The precise measurement of the mixing angle ϕ_τ is of great importance for possible physics beyond the Standard Model, because a non-zero value of ϕ_τ would signify a new type of CP-violating interaction arising from an extended Higgs sector. We have analyzed the impact of future measurements of ϕ_τ and of the $h\tau\tau$ Yukawa coupling strength κ_τ on the parameter spaces of a number of 2-Higgs-doublet extensions of the SM with Higgs-sector CP violation, namely the aligned 2HDM and several conventional 2 HDM with tree-level neutral flavor conservation. Contrary to the information, respectively the constraints which arise from the measurements of the electric dipole moments of atoms/molecules and the neutron, the measurement of ϕ_τ yields direct information on CP-violating neutral Higgs-boson mixing, independent of the mass-values of the other Higgs bosons.

ACKNOWLEDGMENTS

We thank Philipp Bechtle, Klaus Desch, Maike Hansen, Peter Wagner and the members of the $m_{\tau\tau}$ working group of the Helmholtz alliance "Physics at the Terascale" for helpful

discussions. S. B. was supported by B.M.B.F. and S.K. by Deutsche Forschungsgemeinschaft through Graduiertenkolleg GRK 1675.

---

[1] G. Aad et al. (ATLAS Collaboration), Phys.Lett. **B716**, 1 (2012), 1207.7214.

[2] S. Chatrchyan et al. (CMS Collaboration), Phys.Lett. **B716**, 30 (2012), 1207.7235.

[3] V. Khachatryan et al. (CMS), Eur. Phys. J. **C75**, 212 (2015), 1412.8662.

[4] G. Aad et al. (ATLAS) (2015), 1507.04548.

[5] S. Chatrchyan et al. (CMS Collaboration), Phys.Rev.Lett. **110**, 081803 (2013), 1212.6639.

[6] G. Aad et al. (ATLAS Collaboration), Phys.Lett. **B726**, 120 (2013), 1307.1432.

[7] S. Berge, W. Bernreuther, and J. Ziethe, Phys.Rev.Lett. **100**, 171605 (2008), 0801.2297.

[8] S. Berge and W. Bernreuther, Phys.Lett. **B671**, 470 (2009), 0812.1910.

[9] S. Berge, W. Bernreuther, B. Niepelt, and H. Spiesberger, Phys.Rev. **D84**, 116003 (2011), 1108.0670.

[10] R. Harnik, A. Martin, T. Okui, R. Primulando, and F. Yu, Phys.Rev. **D88**, 076009 (2013), 1308.1094.

[11] T. Przedzinski, E. Richter-Was, and Z. Was, Eur. Phys. J. **C74**, 3177 (2014), 1406.1647.

[12] M. J. Dolan, P. Harris, M. Jankowiak, and M. Spannowsky, Phys. Rev. **D90**, 073008 (2014), 1406.3322.

[13] S. Berge, W. Bernreuther, and S. Kirchner, Eur. Phys. J. **C74**, 3164 (2014), 1408.0798.

[14] A. Askew, P. Jaiswal, T. Okui, H. B. Prosper, and N. Sato, Phys. Rev. **D91**, 075014 (2015), 1501.03156.

[15] S. Berge, W. Bernreuther, and H. Spiesberger, Phys.Lett. **B727**, 488 (2013), 1308.2674.

[16] G. Bower, T. Pierzchala, Z. Was, and M. Worek, Phys.Lett. **B543**, 227 (2002), hep-ph/0204292.

[17] K. Desch, Z. Was, and M. Worek, Eur.Phys.J. **C29**, 491 (2003), hep-ph/0302046.

[18] K. Desch, A. Imhof, Z. Was, and M. Worek, Phys.Lett. **B579**, 157 (2004), hep-ph/0307331.

[19] Z. Was and M. Worek, Acta Phys.Polon. **B33**, 1875 (2002), hep-ph/0202007.

[20] M. Worek, Acta Phys.Polon. **B34**, 4549 (2003), hep-ph/0305082.

[21] A. Pich and P. Tuzon, Phys. Rev. **D80**, 091702 (2009), 0908.1554.

[22] A. Rouge, Z.Phys. **C48**, 75 (1990).

[23] M. Davier, L. Duflot, F. Le Diberder, and A. Rouge, Phys.Lett. **B306**, 411 (1993).

[24] J. H. Kuhn, Phys.Rev. **D52**, 3128 (1995), hep-ph/9505303.

[25] A. Stahl, Springer Tracts Mod.Phys. **160**, 1 (2000).

[26] A. van Hameren, Acta Phys. Polon. **B40**, 259 (2009), 0710.2448.

[27] J. A. M. Vermaseren (2000), math-ph/0010025.

[28] A. Buckley, J. Ferrando, S. Lloyd, K. Nordstroem, B. Page, M. Ruefenacht, M. Schoenherr, and G. Watt, Eur. Phys. J. **C75**, 132 (2015), 1412.7420.

[29] B. Gough, *GNU Scientific Library Reference Manual - Third Edition* (Network Theory Ltd., 2009), 3rd ed., ISBN 0954612078, 9780954612078.

[30] R. Brun and F. Rademakers, Nucl. Instrum. Meth. **A389**, 81 (1997).

[31] J. M. Campbell and R. K. Ellis, Nucl. Phys. Proc. Suppl. **205-206**, 10 (2010), 1007.3492.

[32] ATLAS-collaboration, Journal of Instrumentation **3**, S08003 (2008).

[33] ATLAS-collaboration, ATLAS-CONF-2013-108, ATLAS-COM-CONF-2013-095 (2013).

[34] A. Arbey, J. Ellis, R. M. Godbole, and F. Mahmoudi, Eur. Phys. J. **C75**, 85 (2015), 1410.4824.

[35] B. Li and C. E. M. Wagner, Phys. Rev. **D91**, 095019 (2015), 1502.02210.

[36] S. F. King, M. Muhlleitner, R. Nevzorov, and K. Walz (2015), 1508.03255.

[37] G. C. Branco, P. M. Ferreira, L. Lavoura, M. N. Rebelo, M. Sher, and J. P. Silva, Phys. Rept. **516**, 1 (2012), 1106.0034.

[38] S. Dawson et al., in *Community Summer Study 2013: Snowmass on the Mississippi (CSS2013) Minneapolis, MN, USA, July 29-August 6, 2013* (2013), 1310.8361.

[39] M. Jung and A. Pich, JHEP **04**, 076 (2014), 1308.6283.

[40] A. Celis, V. Ilisie, and A. Pich, JHEP **12**, 095 (2013), 1310.7941.

[41] W. Bernreuther, T. Schroder, and T. Pham, Phys.Lett. **B279**, 389 (1992).

[42] E. Accomando et al. (2006), hep-ph/0608079.

[43] O. Eberhardt, U. Nierste, and M. Wiebusch, JHEP **07**, 118 (2013), 1305.1649.

[44] A. Barroso, P. M. Ferreira, R. Santos, and J. P. Silva, Phys. Rev. **D86**, 015022 (2012), 1205.4247.

[45] K. Cheung, J. S. Lee, E. Senaha, and P.-Y. Tseng, JHEP **06**, 149 (2014), 1403.4775.

[46] B. Grzadkowski, O. M. Ogreid, and P. Osland, JHEP **11**, 084 (2014), 1409.7265.

[47] D. Fontes, J. C. Romao, R. Santos, and J. P. Silva, JHEP **06**, 060 (2015), 1502.01720.

[48] S. Inoue, M. J. Ramsey-Musolf, and Y. Zhang, Phys. Rev. **D89**, 115023 (2014), 1403.4257.

[49] D. Fontes, J. C. Romao, R. Santos, and J. P. Silva (2015), 1506.06755.

[50] C.-Y. Chen, S. Dawson, and Y. Zhang, JHEP **06**, 056 (2015), 1503.01114.

[51] C. A. Baker et al., Phys. Rev. Lett. **97**, 131801 (2006), hep-ex/0602020.

[52] J. Baron et al. (ACME), Science **343**, 269 (2014), 1310.7534.

[53] M. Aoki, S. Kanemura, K. Tsumura, and K. Yagyu, Phys. Rev. **D80**, 015017 (2009), 0902.4665.